Physical Thermodynamics Applied to Nano Systems. A short review

Miguel Ángel Sáez Paguay[a*] & María Fernanda Heredia Moyano[b]
[a]Facultad de Recursos Naturales, Escuela Superior Politécnica de Chimborazo (ESPOCH), Orellana 220201, Ecuador
[b]Facultad de Ciencias, Escuela Superior Politécnica de Chimborazo (ESPOCH), Riobamba, 060155, Ecuador

Abstract:
Over the last decades, transition metal nanomaterials have been the subject of numerous investigations for their products due to their wide range of applications. The applicability of thermodynamics to small systems can be investigated by various research methods. In the present work, the Gibbs surface phase method, which can be applied to nanoparticles if the effective surface tension is interpreted as a function of the particle radius, and the Swift heavy-ion irradiation (SHII) method for the shape transformation of induced metal nanoparticles will be analyzed.
Keywords: Nanoparticles; physical properties; physical laws; thermodynamic laws; particle transformation.
DOI: 10.24297/j.cims.2023.22

1. Introduction

The problem of the applicability of thermodynamics to highly dispersed systems is of great interest from both fundamental and practical points of view. Among the most important directions is the extension of the thermodynamics of surface Gibbs phases to dispersing systems. Important contributions to the thermodynamics of highly dispersed systems were made by Gibbs [1]. The interest in the thermodynamics of small objects has increased considerably in view of the rapid development of nanoscience and nanotechnology. The laws of thermodynamics were formulated as phenomenological laws about observable and operationally defined quantities. One of the main points of classical thermodynamics is that the thermodynamic approach is applicable to single macroscopic systems, i.e., systems containing a large number of molecules, atoms, ions, etc. From this point of view, a single small object, including a nanometer droplet and a nanocrystal, does not satisfy the definition of the macroscopic thermodynamic system. At the same time, a set of many small objects will be a macroscopic system [2].

Particularly, the thermodynamic methods analyzed in the present work are promising for the prediction of the stability or instability of nanoparticles. Then, it is shown that the first Gibbs surface phase method has all approaches using the concept of small object (the particle) can be classified into two main directions. The first one consists of studies of the influence of the curvature of the surface tension boundary, i.e., of curvature corrections to the macroscopic value of the surface tension γ. These studies were initiated by Gibbs [1] who concluded that the surface tension γ and the radius change curvature interface R are in the same direction. As a development of the approach outlined by Gibbs and Tolman, who mentions, that the effect of droplet size on surface tension is given theoretical consideration with the help of results from Gibbs' thermodynamic theory of capillarity for the sign and magnitude of surface densities. It is concluded that the surface tension can be expected to decrease with decreasing droplet size over a wide range or circumstances. In addition, approximate figures are obtained for the rate at which such decreases can be expected. The decreases become significant for very small droplets. The results are of interest in view of the important role of surface tension in determining the behavior of small droplets [2].

It is shown that the method of surface Gibbs phases can be extended to nanoparticles if the effective surface tension (the excess specific free energy) is interpreted as a function of the particle radius. The specific surface free energy (the surface tension) for nanodrops and noble gas nanocrystals was calculated using thermodynamic perturbation theory. It has been shown that the average surface tension decreases with particle size for both small droplets and nanocrystals [3].

Also shown is the second method analyzed in this paper, which is the Swift heavy-ion irradiation (SHII) method for the shape transformation of embedded metal nanoparticles using a SiO_2(Silica) base solution. Macroscopically, amorphous SiO_2 $(a-SiO_2)$undergoes anisotropic volume-conserving deformation when subjected to SHII such that thin independent layers contract and expand, respectively, in directions parallel and perpendicular to that of the incident ion [4]. The anisotropy is related to the ion beam direction: materials expand perpendicular to the ion beam and contract parallel to the ion beam while maintaining their volume. Anisotropic deformation is most pronounced at low temperatures 100 K and decreases with increasing irradiation temperature. The deformation increases with ion creep at a constant rate, without saturation. It is well established that the deformation is driven primarily by electronic excitations rather than ion beam induced atomic displacements [5]. The viscoelastic model is a model

describing the ion origin induced by an anisotropic plastic deformation beam is derived and discussed. It is based on a viscoelastic thermal peak model for viscous flow in single ion tracks derived by Trinkaus and Ryazanov. Deviatoric (shear) stresses, caused by rapid thermal expansion of the thermal peak, relax at ion track temperatures beyond a certain driving temperature. Relaxation of shear stress is accompanied by the generation of viscous strains [5,6]. Elemental metal nanoparticles (NPS) embedded in $\alpha - SiO2$ and subjected to SHII can undergo an intriguing shape transformation where the once spherical NPs become progressively more rod-like with the elongation direction aligned along the incident ion. This phenomenon has been reported for several metals under a wide range of SHII conditions. For this report, we examined the SHII-induced elongation of each of ten elemental metal-embedded NPs systems using a common irradiation condition to allow the identification of subtle, metal-specific differences and to demonstrate that the thermodynamic properties of both the matrix and the metal are intrinsic to the shape transformation process [7].

2. Extension of the methods applied to arbitrarily small objects.

In this paper the analysis of the above-mentioned methods was performed independently, starting with the Gibbs Surface Phase method and then with the Swift Heavy Ion Irradiation (SHII) method.

Before explaining the methods mentioned in this article, there will be a brief introduction of some frequently asked questions in our minds, in order to understand the central ideas explained in these methods of application to nanoparticles, such as: How is a nanoparticle, how is a nanoparticle obtained, what form does a nanoparticle have and how is a nanoparticle formed.

What is a nanoparticle?

A nanoparticle of any substance, besides having a small size, is formed by few atoms and an important fraction of them is on its surface, so it has an important energetic role. Creating surface implies creating surface tension, which makes the nanoparticle energetically unstable, a little more unstable than a piece of the same material. Conclusion: nanoparticles are unstable with respect to "bulky" materials, so nanoparticles would ever become large particles, since that leads to having less energy. But it is not so easy for a nanoparticle to grow since it has to incorporate material from somewhere. Some nanoparticles have "shells", which make them more stable, in other cases, to make them grow it is necessary to continuously add material,

which is not always possible. Others must dissolve to give rise to larger nanoparticles and are not always soluble.

How is a nanoparticle obtained?

Nanoparticles are often obtained by very energetic grinding of larger-grained particles, which is very common in the case of ceramics. Other times, nano-objects are generated by etching or lithography methods. Milling methods allow obtaining various materials, they are interesting when there is a very cheap precursor method, but they do not have the fine control offered by "bottom-up" methods.

Shape of nanoparticles

The shape of the nanoparticle has to do with the structure of the material and its growth process. The common salt NaCl, for example, has a compact cubic packing structure (Figure 1). The walls or faces of the cube have an equal number of sodium' s and chlorides and there are diagonal planes containing only sodium' s or chlorides.

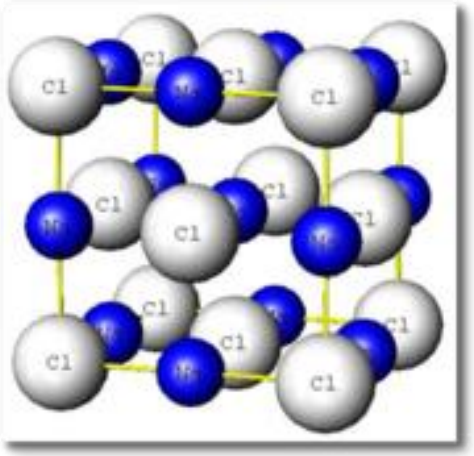

Figure 1. Structure of NaCl.

Let us imagine that a crystal has to grow and that the charged ions in solution can be deposited on the "faces" (electrically neutral) or on the more charged planes. The ions will prefer to deposit on a face with the opposite charge than on a neutral face. Therefore, the "diagonal" faces will grow much faster than the neutral faces and the final shape will be that of a cube. This is a classic case of how the external shape of a crystal reflects the internal arrangement of atoms. This is true for both microscopic size particles and nanoparticles.

In terms of growth, we take zinc oxide, ZnO, as an example, it has a compact hexagonal packing. In Figure 2 we see that the side faces of the prism are "neutral", while the "tops" have alternating layers of positive and negative ions. This makes it easy for it to grow along its vertical axis and tends to form long needles of hexagonal nanometer cross-section.

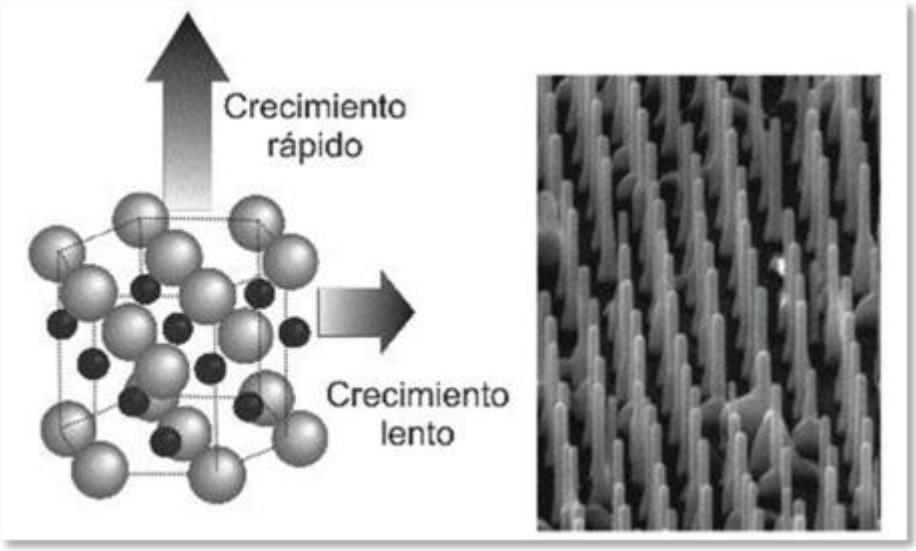

Figure 2. Growth of ZnO nanoparticles.

How is a nanoparticle formed?

To form a nanometric object, you have to gather material, put atoms or ions next to each other, to build a very precise building, more or less large, from a few hundred to a few thousand atoms. Essentially, the formation of a particle is divided into three stages: nucleation, growth and maturation. These stages will determine its composition, shape and size. We have to keep in mind that the formation of a particle implies that the particle is not soluble in the solvent in which it is found or the gas with which it is in contact.

Let us remember three things: that in a saturated solution we cannot dissolve more than one given substance, that a saturated solution is in equilibrium with a solid of that substance, and that the saturation conditions depend in principle on the amount of dissolved matter and on the temperature (at least). Therefore, if we are in a saturated solution and want to make particles, we either add more material or lower the temperature. Either of these two perturbations changes the equilibrium and starts to form particles from the dissolved material in solution. We could also add a precipitating agent, a solid substance that allows us to obtain a solid from a solution. In a supersaturated solution, the solute molecules meet at some point, attract each other and begin to form small clusters or "embryos" of a certain size. Embryos are small, formed by a few

or a few tens of molecules, which come together spontaneously. They are nanometric objects, in which some of the molecules are inside and others are part of a surface. The clusters that are formed have different energies with respect to the molecules in solution. Very small clusters have higher energies than ions in solution because it is bad to create surface area. As they grow, they are very likely to fall apart. Growing is unfavorable until a certain radius is reached, called the critical radius, beyond which, gathering more building units leads to stabilizing the system. In Figure 3 we see that reaching that critical size is a major energy barrier, which, once crossed, facilitates the formation of a particle. From that size, a cluster, which is formed, grows, because its energy decreases with size. These nuclei are the precursors of nanoparticles. The control over the formation of nuclei is very important in the formation of nanoparticles.

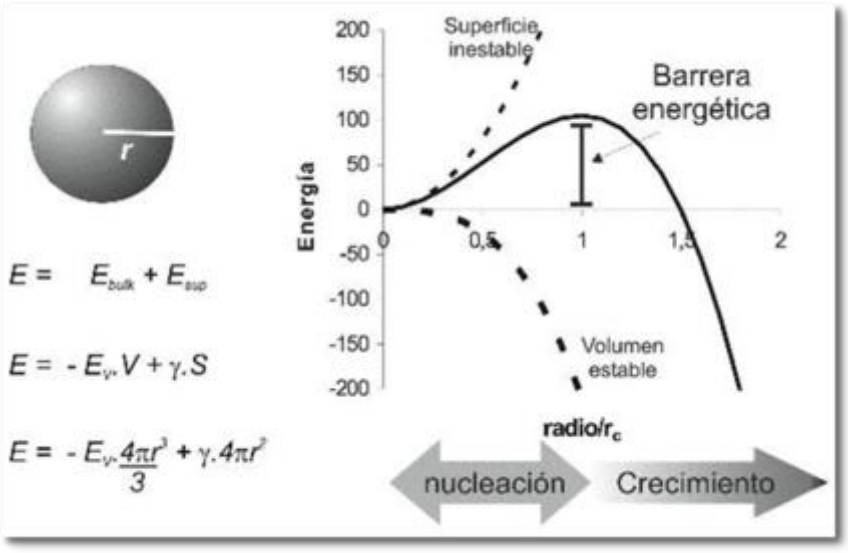

Figure 3. The critical radius of a nanoparticle

2.1. Analysis of the Gibbs Surface Phase Method at arbitrarily small objects.

The work developed by R. Tolman [2] deriving the well-known equation as:

$$\frac{\gamma}{\gamma_\infty} = \frac{1}{1+\frac{2\delta}{R_s}} \qquad (1)$$

Where$\gamma_\infty$is the macroscopic value of the surface tension γ, $R_s$is the radius of the tension surface, δ >0 is the Tolman length defined in [2] as the distance between the equimolecular splitting surface and the tension surface for the planar interface. The tension surface corresponds to the minimum value of the function $\gamma(R)$,, while the equimolecular partition surface is defined as the

surface for which the automatic adsorption (i.e., the excess in the number of molecules in the interfacial region compared to that of the bulk phases extended up to the partition surface) is zero.

According to [7], $\delta \approx a/3$, smaller than the effective molecular diameter a, hence, where $R = R_s \approx R_e$, where R_e, is the radius of the equimolecular splitting surface. Disregarding in (1) all terms smaller than first order, we obtain the asymptotic form (in $R \to \infty$) of the Tolman formula (1).

$$\frac{\gamma}{\gamma_\infty} = 1 - \frac{2\delta}{R} \qquad (2)$$

According to the Gibbs method, the Helmholtz free energy F, the Gibbs free energy G and the other characteristic functions of the heterogeneous two-phase system can be presented in terms as the sum of the volume $(F\ (V), G\ (V))$ and the surface area $(F\ (S), G\ (S))$.

$$F = F^{(V)} + F^{(S)},$$

$$G = G^{(V)} + G^{(S)}, \qquad (3)$$

Where:

$$\psi F^{(V)} = F_1^{(V)} + F_2^{(V)}, .G^{(V)} = G_1^{(V)} + G_2^{(V)}$$

Gibbs assumes that the term ψ is proportional to the surface area A, obtaining the following results.

$$\psi = F - F_1^{(V)} - F_2^{(V)} = G - G_1^{(V)} + G_2^{(V)}$$
$$\psi = \sigma A \qquad (4)$$

Where, σ is the specific surface free energy coinciding with the surface tension γ for the equimolecular splitting surface. If the excess of a free energy ψ is attributed to the small object as a whole instead of to the interface and defined relative to the same volumes $V_1$and V_2 of phases 1 and 2, i.e. its to a small object with the fractal structure can be compared with the volume of a non-fractal bulk phase containing the same number of molecules, then the notion of excess specific free energy σ may be extended to very small particles if σ is defined as ψ/A and, in the general case, interpreted as an effective quantity as a function of particle size and

shape. In the case of low asphericity, when the small object can be adequately characterized by a single geometrical parameter, i.e., by the effective radius R, $\sigma = \sigma\ (R)$.

For single-component systems of crystal vapor and vapor droplets in the vicinity of the melting temperature $N_2 << N_1$. Therefore, R can be defined from the equation $N_1 = {n_1}^{(\infty)}\left(\frac{4}{3}\right) * \pi R^3$ where ${n_1}^{(\infty)}$ is the number of molecules of density in the volume 1 phase. Such a definition of the particle radius R corresponds to the equimolecular splitting surface in the conventional Gibbs method.

2.2. Evaluation of the specific excess free energy of small particles from thermodynamic perturbation theory.

We evaluated on the basis of thermodynamic perturbation theory (TPT) the excess free energy of the small droplet when >> a , obtaining results identical to Tolman's formula $\delta = a/2$.

$$\sigma(R) = \sigma_\infty(1 - a/R) \tag{5}$$

According to TPT, the excess free energy $F - F_0$ (F_0relative to the free energy of a basic unperturbed system can be recognized as the average perturbation energy $\langle \Delta U \rangle$ found on the basis of the unperturbed Gibbs distribution. The simplest illustration of the evaluation of the excess free energy ψ is the case of the small object in the low density medium, in particular, to a droplet or a crystal in the gaseous vapor environment at the temperature $T << Tm$ where Tm is the melting point. In this case:

$$\psi = F - F_0 = G - G_0 = \frac{\langle \Delta U \rangle}{2} \tag{6}$$

Where the perturbation energy $\langle \Delta U \rangle$ is obtained by substituting the infinitely extended reference phase for the volume $V_1 = (4/3) * \pi R^3$ (in the simplest case from the liquid volume or the solid volume in the gaseous vapor medium). It should be noted that for the small object, the number of molecules N becomes a more definite parameter than the radius R of the particle defined from the equation $N = n_\infty(4/3) * \pi R^3$

In the case of a small droplet the reduced averaged perturbation energy $U_{ll}^*$is:

$$\langle U_{ll}^* \rangle = n_l^{*2} \iint_{V_1^* V^* - V_1^*} \Phi^*(r_{12}^*) g(r_{12}^*) dr_1^* dr_2^* \tag{7}$$

Where $g(r_{12}^*)$ is the radial distribution function, r_{12}^* is the reduced distance between points r_1^* and r_2^*; $V_1^* = V_1/a^3$ is the reduced volume of the spherical droplet and V^* is the total volume of the bulk phase in terms of the effective radius potential pair. The expression (7) corresponds to the integration in a six-dimensional space, and the only available method of calculation is Monte-Carlo. Locating the sphere of radius R at the center of the cube with edge L, denoting the total number of random points chosen by M and the number of the attachment points under the hypersurface $-\Phi^*(r_{12}^*)g(r_{12}^*)$ by M_1 we obtain $\langle U_{ll}^* \rangle = -n^{*2}V_1^*(V^* - V_1^*)\left(\frac{M_1}{M}\right)$, where V^* is the reduced volume of the cube with side L^*. The difference $L^* - R^*$must exceed the effective radius of the potential pair. The final formula for $\sigma(R)$ is:

$$\sigma = \frac{2}{3}k\frac{\varepsilon l}{k}n^{*2}\frac{1}{a^2}R^*(L^{*3} - \frac{4}{3}\pi R^{*3})\frac{M_1}{M} \tag{8}$$

With k being the Boltzmann coefficient, but they also demonstrated a simpler application for molecular fluids, as a function of a known radial distribution, such functions yield sufficiently adequate asymptotic values for $\sigma_\infty = \sigma(R)$ of $\sigma(R)$ as can be seen in the figures below.

$$g(r_{12}^*) = \{0,\ para\ \ r_{12}^* < 1\ 1,\ para\ \ r_{12}^* \geq 1 \tag{9}$$

On the other hand, when talking about metal melts, the specific surface free energy σ_∞ depends remarkably or is a function of the radial distribution, that said they showed that for a temperature increase going from the triple point to the critical point, an expression with the following characteristics can be obtained:

$$g(r) = exp\ (-\Phi(r)/kT)\left[1 + \sum_{i=1}^{n} a_i \gamma^{-i}(r,d)/i!\right] \tag{10}$$

The expression in brackets corresponds to the density expansion and the dependent factor (r) of the radial distribution function in the basis function $\underline{\gamma}^i(r,d)$ where d is the effective diameter of the hard sphere. Since this expression in parentheses does not depend on the potential pair $\Phi(r)$, the radial function for molten masses of metal can be expressed in terms of the radial function for the Lennard-Jones system $g_{JL}(r)$ at the same temperature T.

The potential of a Lennard-Jones system consists of a pair of neutral atoms or molecules that are subject to two distinct forces in the limit of large separation and small separation: an attractive

force acting at large distances (Van Der Waals force, or dispersion force) and a repulsive force acting at small distances (the result of overlapping electronic orbitals, known as the Pauli repulsion).

$$g(r)/g_{LJ}(r) = exp\left[-(\Phi(r) - \Phi_{JL}(r))/kT\right] \quad (11)$$

Computational results for the reduced surface tension $\sigma^* = \frac{\sigma(R)}{\sigma_\infty}$ as a function of the reduced Lennard-Jones droplet radius $R^* = \frac{R}{a}$, are presented in Figure. 4.

For Lennard-Jones droplet potential pair parameters: $a = 5.769x10^{-10}m$ and $\varepsilon/k = 345K$, which correspond to n-pentane, were used. As can be seen in Fig. 1, the results are in agreement with formulas (1) and (3). However, the calculated values of σ_∞ for all molecular fluids were overestimated. For aluminum, droplets melt at the melting temperature.
It is also observed that, contrary to the Tolman length δ, the calculated values of the parameters K and σ_∞ agree in order of magnitude with the available experimental data. It should be noted that the experimental values of the δ obtained in [7] on the basis of an indirect and rather complex method may not always be quite reliable. In fact, the approximate but sufficient estimate by Rowlinson and Widom [6] translates into the simple correlation $= 1.12 * \frac{a}{3}$ between δ and a, which gives for n-pentane the value $2.2x10^{-10}m$.

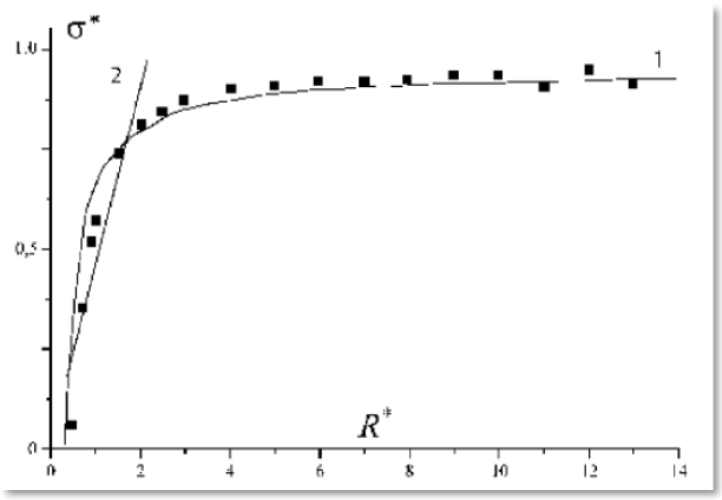

Figure 4. The dependence $\sigma^*(R^*)$ for nanodroplets of the simple Lennard-Jones fluid: 1- the Tolman formula (1) with the parameter δ found from the results of our computer calculations, 2- the linear Rusanov formula (3).

According to the results presented above, the size dependence of the surface tension for small objects of different nature has, in general, the same shape corresponding to curve 1 in Fig. 5. On the other hand, the reduced size dependences $\sigma^*(R^*)$ practically coincide if the linear parameter, i.e., the effective molecular or ionic diameter is chosen appropriately.

The main distinction between curves 1 and 2 is that curve 2 has a maximum. On the one hand, this is of interest and results mostly in the negativity of the Tolmen length δ for the tail of the $\sigma(R)$ curve. On the other hand, the maximum mentioned above is very small, at least for nanodrops. More importantly, the excess specific free energy $\sigma(R)$ is considerably reduced, following the linear Rusanov formula (3) for R smaller than some critical value Rc. Therefore, the size dependence of the surface tension can be approximated by two rectilinear segments, as follows:

$$\sigma(R) = \{KR,\ \ R < R_c\ \sigma_\infty,\ \ R \geq R_c\ \} \tag{12}$$

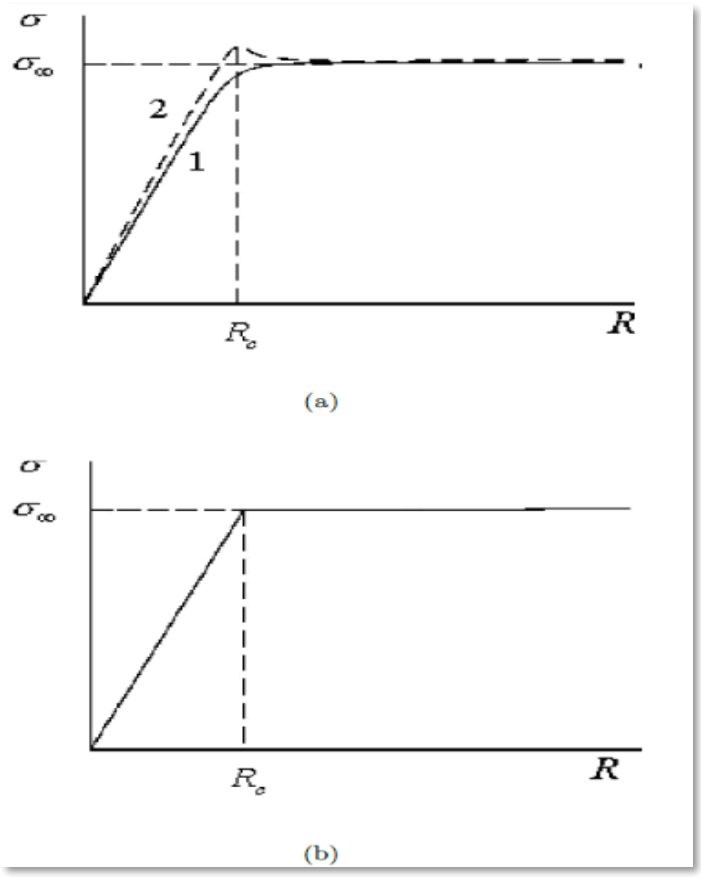

Figure 5. available types of theoretical dependencies for σ(R) (a) and its simplest approximation (b).

In $R \geq Rc$ only the small object can be treated as a self-contained thermodynamic phase containing a central core corresponding to the bulk phase structure. In $R < Rc$, the agranel and surface areas cannot be separated in the object under consideration, i.e., the particle under consideration becomes a kind of 'surface object'.

2.3. Analysis of the Swift heavy-ion irradiation (SHII) method.

This method can be termed as the ion-solid interaction during swift heavy-ion irradiation (SHII) is dominated by inelastic processes in the form of electron excitation and ionization while, on the contrary, the influence of elastic processes such as ballistic displacements is negligible. For the process of obtaining results of the fast heavy ion irradiation method, amorphous SiO_2 (SiO_2) is macroscopically analyzed and subjected to anisotropic volume-conserving deformation when subjected to SHII such that the thin independent layers contract and expand, respectively, in directions parallel and perpendicular to that of the incident ion [4]. The viscoelastic model [5,6], on the basis of a transient thermal effect, successfully explains this so-called ion hammering shape.

Microscopically, energy is deposited along the ion path, the incident ion from the electron array is then dissipated within a narrow cylinder of material surrounding the ion path. The heat flow in both electron and lattice subsystems is well described as functions of time and radial distance by the inelastic peak thermal $(i - TS)$ model [8].

When the lattice temperature exceeds that required for melting, the material along the ion path is melted and an ion track is formed by quenching, data demonstrating that the ion-track diameter melted in a SiO_2 as a function of electron braking power. The radial ion-track density distribution consisted of a low-density and high-density shell core (relative to the non-irradiated material), the formation of which was attributed to an inactive pressure wave emanating from the ion-track center [9].

Elemental metal nanoparticles (NPS) embedded in un- SiO_2 are subjected to SHII which can undergo an intriguing shape transformation where the once spherical NPs become progressively more rod-like with the elongation direction aligned along that of the incident ion. This phenomenon has been reported for several metals under a wide range of SHII conditions. Independent metal NPs irradiated under comparable conditions do not change shape,

demonstrating the SiO_2 embedded matrix must play a role in the shape transformation process. An unequivocal identification of the underlying atomistic mechanism of the transformation remains scarce, but a process of melting and flow of metal NPs, the latter potentially as a means of relieving in-plane stress within the matrix, is certainly plausible. In this report, we discuss the examination of SHII-induced elongation of ten each embedded, elemental metal NP systems using a common irradiation condition to enable the identification of subtle, metal-specific differences and demonstrate that the thermodynamic properties of both the matrix and the metal are intrinsic to the shape transformation process.

Elemental metal nanoparticles of Co, Ni, Cu, Zn, Ag, Sn, Pt, Au, Pb, and Bi were formed at a depth of $0.2{\sim}1.5\,mn$ in a $2nm$ thick SiO_2 layer on a crystalline Si substrate by ion implantation and thermal annealing. The processing conditions were necessarily metal specific, but generally yielded a metal concentration of 2-10 % . After implantation and a broad distribution of NPs sizes after annealing. All NPs were approximately spherical in shape, independent of metal species. The samples were then irradiated at room temperature and normal incidence with $185\ MeV\ Au^{+13}$ ions where the electronic braking power in SiO_2 is about $17\ keV/nm$.

The shape transformation was characterized with cross-sectional transmission electron microscopy (XTEM) measurements of lower and higher-dimensional NPs $(d_{min}\ y\ d_{maj}, respectivamente)$or, equivalently, NP width and length. For statistical reliability, approximately $\sim 500\ NPs$ were measured per sample. As an example, Fig. 6 shows XTEM images of Ni, Cu and Bi NPs following SHII where the once spherical metal NPs are elongated in the incident ion direction as expected.

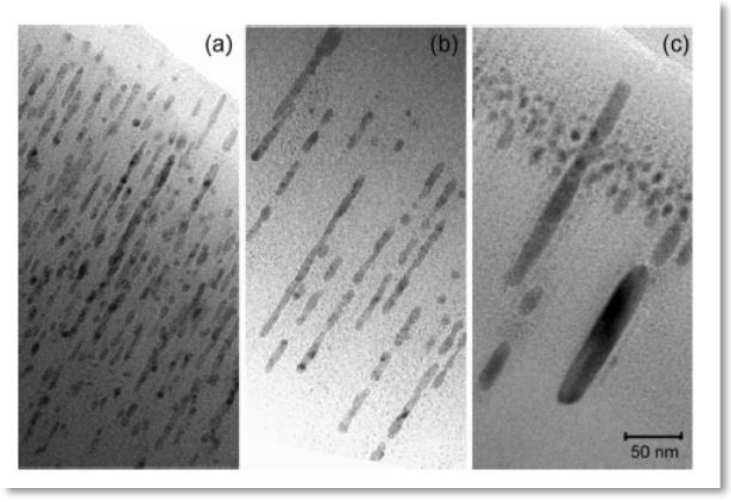

Figure 6. XTEM images of (a) Ni, (b) Cu and (c) Bi. SHII-induced NPs. The incident ion direction was from the upper right to the lower left of the image.

The transformation from spherical to rod shape has not been reported previously for these three metals and therefore such results further demonstrate that SHII-induced shape transformation is operative over a wide range of composition and crystallography of metal NPs embedded in a SiO_2.

For an incident ion intersecting a spherical metal NPs of radius $\frac{d_{min}}{2}$ $(=\frac{d_{maj}}{2})$, the energy density deposited per atom $(E_{dep(sphere)})$ within the NP is:

$$E_{dep(sphere)} = \frac{\varepsilon l}{\frac{4}{3}\pi\left(\frac{d_{min}}{2}\right)^2\left(\frac{d_{maj}}{2}\right)N} \tag{13}$$

Where ε and l are the electronic ion energy loss in the NP and path length in the NP, respectively, and N is the atomic density. (It should be emphasized that the authors assumed that all energy is deposited along the ion path, showing that in the bulk material $> 85\%$ of the energy is deposited within $5\,nm$ of the ion-track center for the ten metals under consideration. Furthermore, the potential barrier at the confines of the metal/ SiO_2 interface energy electrons $< 4-5\,eV$ to the metal and therefore to a good approximation the energy deposited in the NP remains within the NP). If the ion intersects an NP at a distance B from the NP l-axis, it is given by:

$$l = 2\frac{d_{maj}}{d_{min}}\sqrt{\left(\frac{d_{min}}{2}\right)^2 - B^2} \tag{14}$$

Thus, the deposited energy will be:

$$E_{dep(sphere)} = \frac{12\varepsilon}{\pi(d_{min})^3 N}\sqrt{\left(\frac{d_{min}}{2}\right)^2 - B^2} \tag{15}$$

When a sufficient fraction of $E_{dep(sphere)}$) is transferred to the lattice metal for vaporization, the NPs vaporize and dissolve in the matrix. Clearly the $E_{dep(sphere)}$ is given as approximately $(\frac{1}{d_{min}^2})$

and, for any given metal, therefore for smaller NPs are more susceptible to vaporization than their larger counterparts. As the dissolved metal and matrix atoms cool, then the metal atoms may remain dispersed in the matrix, forming new clusters and/or be absorbed by more stable larger NPs.

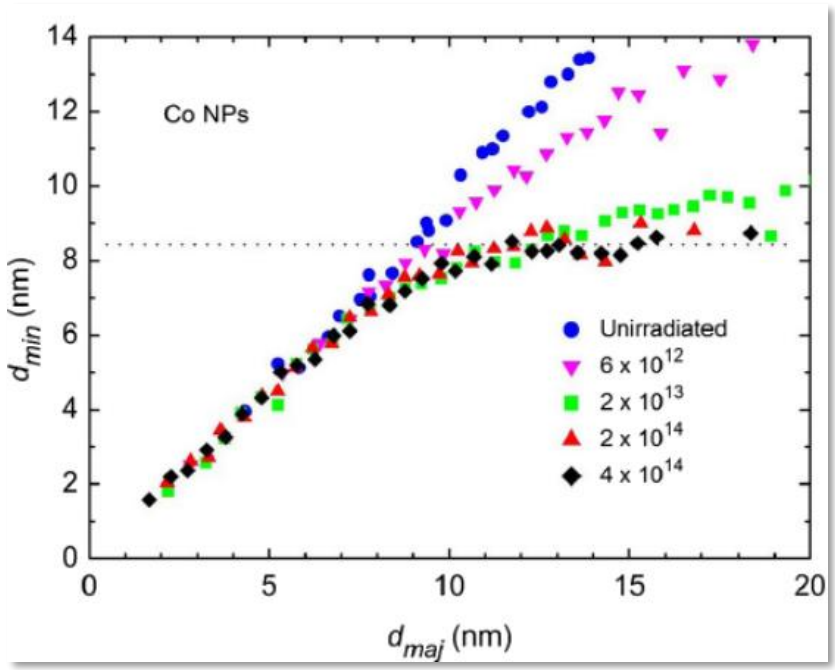

Figure 7. (Colored lines). NP elongated width (dmin) as a function of NP elongated length (dmaj) following SHII of Co NPs.

For spherical NPs of $diameter > d_{umb.}$, Figure 7 demonstrates the shape transformation proceeding gradually as a function of irradiance fluence with the slope beyond the minimum size threshold progressively close to zero. The latter indicates that all elongated NPs eventually reach a common width independent of their length suggesting that this $d_{min\,(saturation)}$ is a characteristic parameter for SHII elongated NPs. The $d_{min\,(saturation)}$ values were determined for the ten different metals and, to better relate these data to the thermodynamic properties of both the metal and the matrix, the results are plotted in Fig. 8 as a function of the energy density per atom required to vaporize (E_{vap}) the bulk metal.

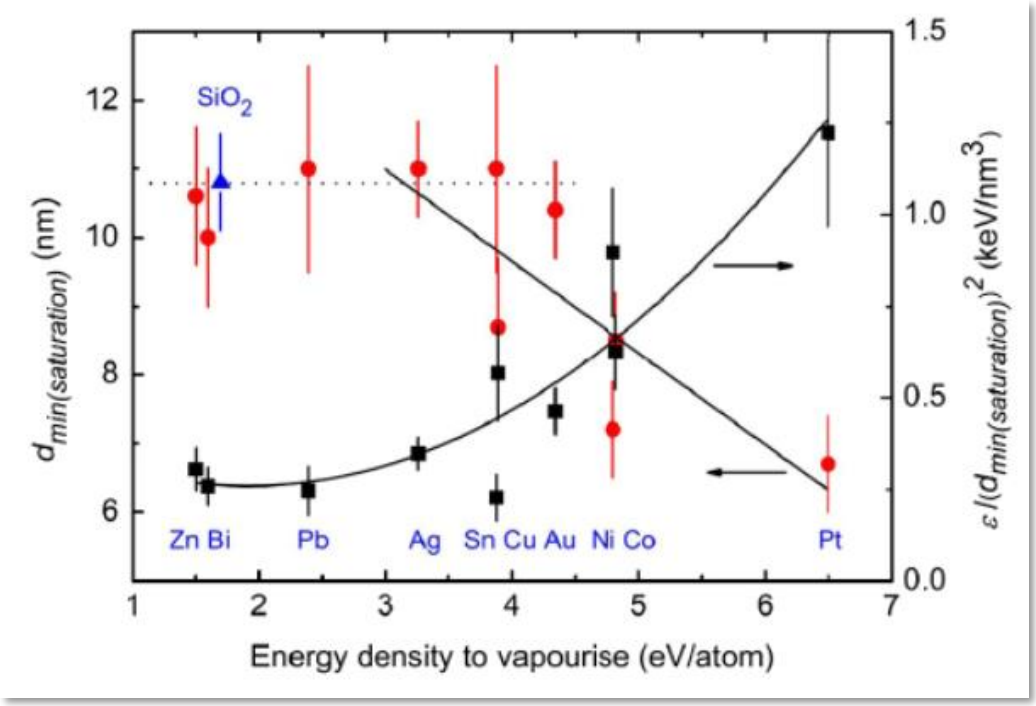

Figure 8. (Color line). Saturated width NP $d_{min\ (saturation)}$ and $\frac{\varepsilon}{(d_{min\ (saturación)})^2}$ as a function of the energy density per atom required for vaporization. The horizontal line is the fused ion-track diameter in a-SiO_2 and the associated experimental uncertainty is indicated by the error bars in the triangular symbol.

With reference to Fig. 8, two distinct trends are evident: $(d_{min\ (saturación)})$ is effectively constant at low (E_{vap}) then decreases approximately linearly at higher values. In summary, this work deals with the investigation of SHII-induced shape transformation in a variety of elemental metal NPs embedded in a SiO_2. Spherical NPs below a threshold diameter do not elongate, while those of larger size progressively transform to a bar-like shape of fixed width independent of length. Using a common irradiation condition allowed us to identify differences in metal-specific spherical NPs at both the threshold diameter and elongated NP width and relate these differences to the width of the molten ion track in a SiO2 and the energy density per atom required for metal NP vaporization. Spherical NPs below the threshold diameter for elongation and elongated NPs below the saturation width are unstable under SHII and vaporize as a result of interaction with an incident ion. While this defines the minimum sustainable width of an elongated NPs, the maximum is limited to the width of the ion track in a SiO_2 within which the molten metal flows.

3. Conclusions

Thermodynamics applied to Nanoparticles analyzed in the present work are promising for the prediction of nanoparticle stability or instability.

Gibbs thermodynamics can be extended to nanometer-sized objects, if the size dependence of the surface tension or excess specific free energy is properly taken into account.

The method of surface Gibbs phases can be extended to nanoparticles if the effective surface tension (the specific excess free energy) is interpreted as a function of the particle radius.

Nanoparticles when subjected to SHII such that the thin independent layers contract and expand, respectively, in directions parallel and perpendicular to that of the incident ion, i.e. are able to take an elongated shape.

Nanoparticles induced by SHII on an elemental metal embedded in a SiO2 elongate into rod-like shapes depending on the size of the threshold diameter.

Acknowledgments

The authors would like to thank all the researchers of the Physics Department of ESPOCH, who in one way or another contributed in a disinterested way with their good comments for the completion of this work.

References

1. T.L. Hill, Thermodynamics of Small Systems: Part 1, Thermodyn. Small Syst. Part 1. 3182 (1963). https://doi.org/10.1063/1.1732447.
2. R.C. Tolman, The Effect of Droplet Size on Surface Tension, J. Chem. Phys. 17 (1949) 333. https://doi.org/doi:10.1063/1.1747247.
3. V.M. Samsonov, a. N. Bazulev, N.Y. Sdobnyakov, On applicability of Gibbs thermodynamics to nanoparticles, Cent. Eur. J. Phys. 1 (2003) 474–484. https://doi.org/10.2478/BF02475858.
4. A. Benyagoub, S. Klaumünzer, M. Toulemonde, Radiation-induced compaction and plastic flow of vitreous silica, Nucl. Instruments Methods Phys. Res. Sect. B Beam Interact. with Mater. Atoms. 146 (1998) 449–454. https://doi.org/10.1016/S0168-583X(98)00478-9.

5. T. Van Dillen, a. Polman, P.R. Onck, E. Van Der Giessen, Anisotropic plastic deformation by viscous flow in ion tracks, Phys. Rev. B - Condens. Matter Mater. Phys. 71 (2005) 1–12. https://doi.org/10.1103/PhysRevB.71.024103.
6. H. Trinkaus, a. Ryazanov, Viscoelastic Model for the Plastic Flow of Amorphous Solids under Energetic Ion Bombardment, Phys. Rev. Lett. 74 (1995) 5072–5075. https://doi.org/10.1103/PhysRevLett.74.5072.
7. M.C. Ridgway, R. Giulian, D.J. Sprouster, P. Kluth, L.L. Araujo, D.J. Llewellyn, a. P. Byrne, F. Kremer, P.F.P. Fichtner, G. Rizza, H. Amekura, M. Toulemonde, Role of thermodynamics in the shape transformation of embedded metal nanoparticles induced by swift heavy-ion irradiation, Phys. Rev. Lett. 106 (2011). https://doi.org/10.1103/PhysRevLett.106.095505.
8. M. Toulemonde, C. Dufour, E. Paumier, Transient thermal process after a high-energy heavy-ion irradiation of amorphous metals and semiconductors, Phys. Rev. B. 46 (1992) 14362–14369. https://doi.org/10.1103/PhysRevB.46.14362.
9. P. Kluth, C.S. Schnohr, O.H. Pakarinen, F. Djurabekova, D.J. Sprouster, R. Giulian, M.C. Ridgway, a. P. Byrne, C. Trautmann, D.J. Cookson, K. Nordlund, M. Toulemonde, Fine structure in swift heavy ion tracks in amorphous SiO2, Phys. Rev. Lett. 101 (2008) 1–4. https://doi.org/10.1103/PhysRevLett.101.175503.